2018

Exchange-Coupled $Fe_3O_4/CoFe_2O_4$ Nanoparticles for Advanced Magnetic Hyperthermia

Josue Robles
University of South Florida, jrobles@usf.edu

R. Das
University of South Florida

M. Glassell
University of South Florida

Manh-Huong Phan
University of South Florida, phanm@usf.edu

Hariharan Srikanth
University of South Florida, sharihar@usf.edu

Exchange-coupled $Fe_3O_4/CoFe_2O_4$ nanoparticles for advanced magnetic hyperthermia

Cite as: AIP Advances **8**, 056719 (2018); https://doi.org/10.1063/1.5007249
Submitted: 01 October 2017 . Accepted: 19 November 2017 . Published Online: 05 January 2018

J. Robles, R. Das, M. Glassell, M. H. Phan, and H. Srikanth

Exchange-coupled $Fe_3O_4/CoFe_2O_4$ nanoparticles for advanced magnetic hyperthermia

J. Robles,[1] R. Das,[1,a] M. Glassell,[1,2] M. H. Phan,[1] and H. Srikanth[1,a]
[1]*Department of Physics, University of South Florida, Tampa, FL 33620, USA*
[2]*Department of Physics and Electrical Engineering, University of Scranton, Scranton, PA 18510, USA*

(Presented 8 November 2017; received 1 October 2017; accepted 19 November 2017; published online 5 January 2018)

We report a systematic study of the effects of core and shell size on the magnetic properties and heating efficiency of exchange-coupled $Fe_3O_4/CoFe_2O_4$ core/shell nanoparticles. The nanoparticles were synthesized using thermal decomposition of organometallic precursors. Transmission electron microscopy (TEM) confirmed the formation of spherical Fe_3O_4 and $Fe_3O_4/CoFe_2O_4$ nanoparticles. Magnetic measurements showed high saturation magnetization for the nanoparticles at room temperature. Increasing core diameter (6.4±0.7, 7.8±0.1, 9.6±1.2 nm) and/or shell thickness (~1, 2, 4 nm) increased the coercive field (H_C), while an optimal value of saturation magnetization (M_S) was achieved for the Fe_3O_4 (7.8±0.1nm)/$CoFe_2O_4$ (2.1±0.1nm) nanoparticles. Magnetic hyperthermia measurements indicated a large increase in specific absorption rate (SAR) for 8.2±1.1 nm $Fe_3O_4/CoFe_2O_4$ compared to Fe_3O_4 nanoparticles of same size. The SAR of the $Fe_3O_4/CoFe_2O_4$ nanoparticles increased from 199 to 461 W/g for 800 Oe as the thickness of the $CoFe_2O_4$ shell was increased from 0.9±0.5 to 2.1±0.1 nm. The SAR enhancement is attributed to a combination of the large M_S and the large H_C. Therefore, these $Fe_3O_4/CoFe_2O_4$ core/shell nanoparticles can be a good candidate for advanced hyperthermia application.
https://doi.org/10.1063/1.5007249

I. INTRODUCTION

Cancer has become one of the most common causes of death in our society, becoming the second leading cause of death in the USA.[1] For this reason, there is a pressing need to improve and find new supplementary ways for cancer treatments that are less toxic than chemotherapy and relatively easy to administer to patients. Magnetic hyperthermia has emerged as a promising candidate for cancer treatment.[2,3] By subjecting magnetic nanoparticles to DC and AC magnetic fields, the location of a tumor can be targeted and doses of heat can be delivered to the cancer cells, respectively, without damaging the surrounding healthy tissues.[2,3] In order to implement this treatment, small concentrations of nanoparticles with high heating efficiency are desired.[4,5] For biomedical applications, iron oxide nanoparticles are commonly used due to their intrinsic biocompatibility.[6,7] In particular, Fe_3O_4 and γ-Fe_2O_3 nanoparticles have been extensively studied for magnetic hyperthermia because of their tunable magnetic properties and stable suspension in the superparamagnetic regime. However, their relatively low heating capacity or small specific absorption rate (SAR) makes them less desirable for practical applications.[8,9] It has been shown that the SAR of magnetic nanoparticles can be tuned by varying particle size, saturation magnetization, and effective anisotropy.[6,7,10,11] Recently, a large improvement in SAR has been reported in exchange-coupled nanoparticles with exchange coupling between soft and hard magnetic phases.[12,13] However, the origin of the magnetic exchange-enhanced

[a]Corresponding authors: rajadas@usf.edu (R.D.); sharihar@usf.edu (H.S.)

heating efficiency and the effect of core diameter and shell thickness on the heating efficiency in these systems have remained unclear and unexplored.

In the present study, we report how the variations in the core diameter and shell thickness affect the magnetic response and heating efficiency of exchange-coupled $Fe_3O_4/CoFe_2O_4$ core/shell nanoparticles.

II. EXPERIMENT

Fe_3O_4@$CoFe_2O_4$ nanoparticles of varying core diameter (6.4±0.7, 7.8±0.1, 9.6±1.2 nm) and shell thickness (~1 nm, 2 nm, and 4 nm) were prepared by seed mediated thermal decomposition of organometallic precursors in the presence of oleic acid, oleylamine, 1-2, hexadecanediol, and benzyl ether. The details of the synthesis process are described elsewhere.[14,15] A Bruker AXS D8 X-ray diffractometer (XRD) was used to analyze the crystalline structure of the nanoparticles. Transmission electron microscopy (TEM, FEI Morgagni 268, 60kV) was performed in order to obtain the shape and size distribution of the nanoparticles. The magnetic properties of the nanoparticles were measured using a Physical Property Measurement System (PPMS) from Quantum Design, with a vibrating sample magnetometer insert. Magnetic hysteresis (M-H) loops were performed at 300K with applied fields ranging from -50 to 50 kOe. Saturation magnetization of the particle samples was normalized by the mass of the dried particles used for the measurement. The contribution of surfactant mass to the final mass of the dried particles is not significant to change the accuracy of the saturation magnetization. AC magnetic hyperthermia experiments were carried out using a 4.2 kW Ambrell Easyheat LI 3542 system. The frequency was fixed at 310 kHz and the amplitude of the magnetic field was adjusted from 400 to 800 Oe. During the hyperthermia experiments, the particles were dispersed in hexane with a concentration of 1mg/ml.

III. RESULTS AND DISCUSSION

Figure 1 shows the TEM images of Fe_3O_4 cores and $Fe_3O_4/CoFe_2O_4$ core/shell nanoparticles. From TEM, the nanoparticles are observed to have a roughly spherical shape. As mentioned above, the $Fe_3O_4/CoFe_2O_4$ nanoparticles were obtained using a seed mediated thermal decomposition process. In this process, a Fe_3O_4 seed nanoparticle was used as a template in order to grow the $CoFe_2O_4$ shell. To obtain various shell thicknesses, the previous synthesis process was repeated using the core/shell nanoparticle as a seed. Using this synthesis method, we observed an increment in the nanoparticle size by ~2 nm, excluding the case for Figure 1(f) where we saw an increment of ~4 nm (Table I). The thickness of the shell was determined by measuring the particles size before and after the seed-mediated shell growth.

XRD measurements were performed to confirm the composition and crystal structure of the nanoparticles. Figure 2 shows the XRD patterns for the 6.4±0.7 nm Fe_3O_4 core and the 6.4±0.7 nm/ 0.9±0.5 nm $Fe_3O_4/CoFe_2O_4$ core/shell nanoparticles. The XRD patterns possess six distinctive peaks for Fe_3O_4 and $CoFe_2O_4$ nanoparticles. The peak positions correspond to the cubic structure of an iron phase that can be either magnetite or maghemite.[16] Here we note that XRD alone is not a conclusive tool to distinguish between Fe_3O_4 and $CoFe_2O_4$ phases due to their similar structure.

Magnetic measurements were performed on the nanoparticles to understand their magnetic properties and effects on the heating efficiency. It is well known that there is a correlation between the heating efficiency and the saturation magnetization of the nanoparticles.[17] All the measurements were conducted at room temperature (same temperature as hyperthermia measurements). In order to see how the magnetization evolves in the core/shell system, hysteresis loops were taken for various core diameters and shell thicknesses. Figure 3(a) shows the M-H loops for different core/shell systems, where the core diameter remained the same (7.8±0.1 nm) and the shell thickness was varied from ~1 to 4 nm. It can be seen from Figure 3(a) that the saturation magnetization (M_S) increases as the $CoFe_3O_4$ shell thickness increases, until a critical thickness (2.1±0.1 nm) is reached. On the other hand, when the core diameter was varied from 6.4±0.7 to 9.6±1.2 nm and the shell thickness remained the same (~1 nm), M_S remained constant until the diameter of the core reached 7.8±0.1 nm, above which we observed an increase in M_S (see Figure 3(b)). In the case where the shell thickness was

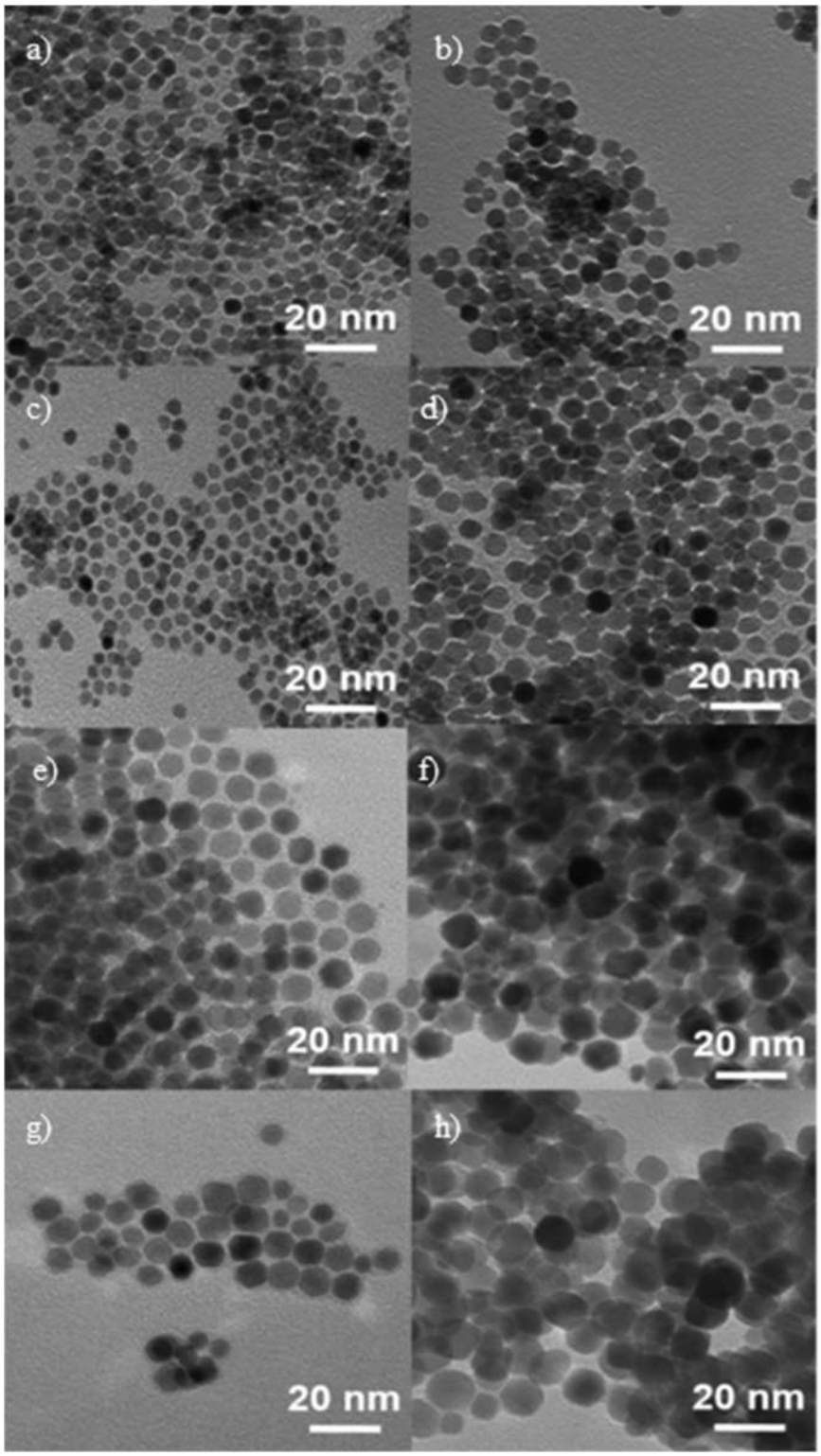

FIG. 1. TEM images of Fe_3O_4 core and $Fe_3O_4/CoFe_2O_4$ core/shell nanoparticles: a) 6.4±0.7 nm core, b) 6.4±0.7 nm/ 0.9±0.5 nm, c) 7.8±0.1 nm core, d) 7.8±0.1 nm/0.9±0.3 nm, e) 7.8±0.1 nm/2.1±0.1 nm, f) 7.8±0.1 nm/4.4±1.1 nm, g) 9.6±1.2 nm core, h) 9.6±1.2 nm/1.4±0.4 nm.

varied, the highest M_S (~83 emu/g) obtained corresponds to the ~2 nm shell thickness, while for the ~1 nm and ~4 nm shell systems, M_S remained at ~68 emu/g. For the case where the core diameter was varied, however, the highest M_S (~76 emu/g) was obtained for the system with a core diameter

TABLE I. Fe_3O_4 core diameter, $CoFe_2O_4$ shell thickness, coercive field (H_C), saturation magnetization (M_S), and specific absorption rate (SAR).

Fe_3O_4 core size (nm)	$CoFe_2O_4$ shell thickness (nm)	Coercive field, H_C (Oe)	Saturation magnetization, M_S (emu/g)	Specific absorption rate, SAR (W/g)
6.4±0.7(6)	0	0	46	5
	0.9±0.5(1)	0	67	208
7.8±0.1(8)	0	0	58	8
	0.9±0.3(1)	0	68	199
	2.1±0.1(2)	123	83	461
	4.4±1.1(4)	500	68	129
9.6±1.2(10)	0	0	54	12
	1.4±0.4(1)	324	76	174

of 9.6±1.2 nm, while for the 6.4±0.7 nm and 7.8±0.1 nm core diameter samples M_S remained around 67-68 emu/g (Table I). The 6.4±0.7, 7.8±0.1, and 9.6±1.2 nm Fe_3O_4 core, 6.4±0.7 nm/0.9±0.5 nm, and 7.8±0.1 nm/0.9±0.3 nm core/shell nanoparticles showed a superparamagnetic behavior (coercive field, $H_C \sim 0$ Oe) at room temperature, while the other core/shell NPs showed considerable values of H_C (Table I). The increase of H_C in core/shell $Fe_3O_4/CoFe_2O_4$ compared to Fe_3O_4 nanoparticles of same size can be attributed to the exchange interaction between the soft Fe_3O_4 core and the hard $CoFe_2O_4$ shell.[7,12]

The heating efficiency of the nanoparticles was calculated using the specific absorption rate (SAR), which is expressed as follows:

$$SAR = \frac{\Delta T}{\Delta t} \times C_p \times \frac{m_s}{m_n}$$

where C_p is the specific heat of the solution, m_s the mass of the solution, m_n the mass of the nanoparticles, and $\Delta T/\Delta t$ is the initial slope of the heating curve. Figure 4 shows SAR vs. field for the core/shell nanoparticles with various core diameters and shell thicknesses. As can be observed, SAR increased with increasing the AC magnetic field, except for the 7.8±0.1 nm core where the SAR value was negligible in comparison to the other systems. The highest SAR value (~461 W/g) was observed at 800 Oe for the 7.8±0.1 nm/2.1±0.1 nm core/shell nanoparticles. Also, the 7.8±0.1 nm/0.9±0.3 nm and 6.4±0.7 nm/0.9±0.5 nm core/shell nanoparticles showed similar SAR values when increasing the AC magnetic field. The SAR enhancement of the 7.8±0.1 nm/2.1±0.1 nm $Fe_3O_4/CoFe_2O_4$ core/shell nanoparticles can be attributed to the exchange coupling between the core and shell, which, in turn,

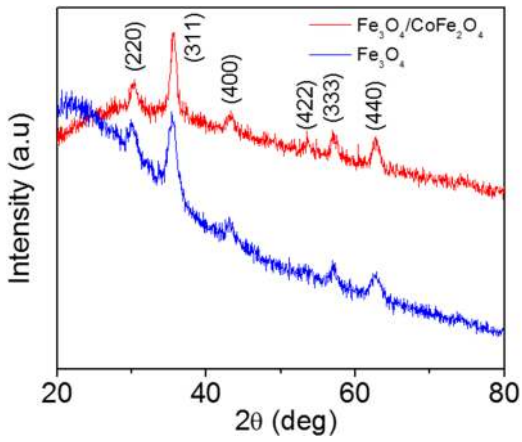

FIG. 2. XRD patterns of Fe_3O_4 core and $Fe_3O_4/CoFe_2O_4$ core/shell nanoparticles.

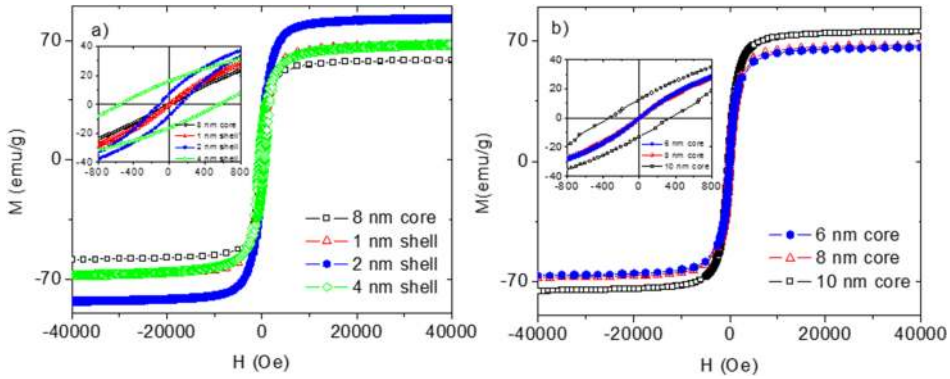

FIG. 3. M-H loops of $Fe_3O_4/CoFe_2O_4$ core/shell nanoparticles: a) The same core diameter (7.8±0.1 nm) but different shell thicknesses, b) the same shell thickness but different core diameters. Insets a), b) show the low field region of M-H loops.

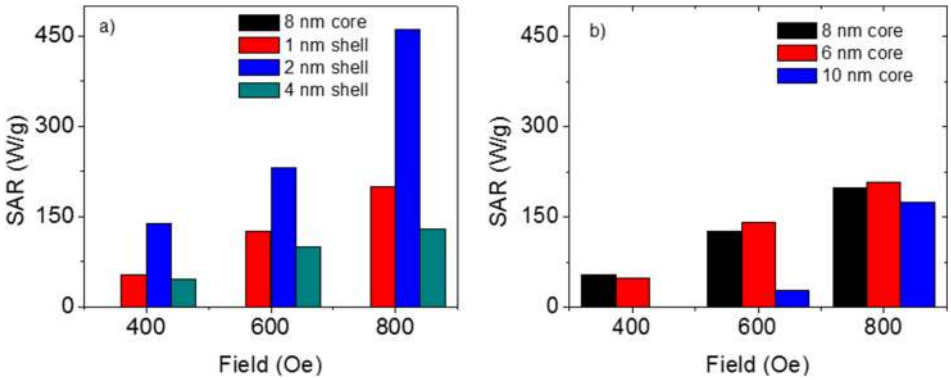

FIG. 4. SAR values for $Fe_3O_4/CoFe_2O_4$ core/shell nanoparticles: a) the same core diameter (7.8±0.1 nm) with different shell thicknesses, b) the same shell thickness (~1 nm) but different core diameters.

increases in coercive field, H_C (Table I) and effective magnetic anisotropy, H_K.[18] It is worth mentioning that the increase in the SAR value is greater for the variation of the shell thickness than the variation in the core diameter. From these observations, we can infer that the increase in SAR is governed largely by the shell thickness in these nanoparticles. Moon *et. al.* also showed that for $CoFe_2O_4/Fe_3O_4$ core/shell nanoparticles, thinner shells of Fe_3O_4 (~1-2 nm) play a significant role in enhancing the magnetic anisotropy (surface anisotropy) of the system, thus increasing the SAR values.[13] In the case of $Fe_3O_4/CoFe_2O_4$ core/shell nanoparticles, we found the enhancements of H_C and H_K with increase in $CoFe_2O_4$ shell thickness, using the transverse susceptibility (TS) technique.[18] The lower SAR values for the 9.6±1.2 nm/1.4±0.4 nm and 7.8±0.1 nm/4.4±1.1 nm core/shell nanoparticles can be attributed to the lower M_S (see M-H loops) and the fact that bigger nanoparticles tends to agglomerate.[16,19] The magnetic and hyperthermia parameters of the samples are summarized in Table I.

IV. CONCLUSIONS

We have successfully synthesized $Fe_3O_4/CoFe_2O_4$ core/shell nanoparticles with different core diameters and shell thicknesses. We have studied how the magnetic properties and heating efficiency change when the core and shell sizes are varied and performed a comparative analysis. Our work shows the ability to tune the saturation magnetization and magnetic anisotropy, thus improving the heating efficiency. The results indicate that the variation in the shell thickness has a greater impact on the magnetic response and heating efficiency compared to the variation in the core size in the

$Fe_3O_4/CoFe_2O_4$ core/shell structures. Controlling the core/shell structure of the nanoparticles to tune and improve the magnetic properties and SAR values makes this type of system a promising candidate for advanced hyperthermia applications.

ACKNOWLEDGMENTS

Research at the University of South Florida was supported by the U.S. Department of Energy, Office of Basic Energy Sciences, Division of Materials Sciences and Engineering under Award No. DE-FG02-07ER46438. Joshua Robles acknowledges the financial support provided by the NSF Florida-Georgia Louis Stokes Alliance for Minority Participation (FGLSAMP) through award number HRD #1612347.

[1] American Cancer society, *Cancer Facts & Figures 2017* (American Cancer Society, Atlanta, GA, 2017).
[2] D. Ortega and Q. Pankhurst, "Magnetic hyperthermia," in *Nanoscience: Volume 1: Nanostructure Through Chemistry* (Royal Society of Chemistry, Cambridge, 2013), p. 60.
[3] C. Binns, "Magnetic nanoparticle hyperthermia treatment of tumours," in *Nanostructured Materials for Magnetoelectronics* (Springer-Verlag, Berlin, 2013), p. 197.
[4] S. Dutz and R. Hergt, Int. J. Hyperthermia **29**, 790 (2013).
[5] R. Hergt, S. Dutz, R. Muller, and M. Zeisberger, J. Phys.: Condens. Matter **18**, S2919 (2006).
[6] H. Khurshid *et al.*, J. Appl. Phys. **117**, 17A337 (2015).
[7] S. H. Noh *et al.*, Nano Lett. **12**, 3716 (2012).
[8] Z. Nemati, J. Alonso, H. Khurshid, M. H. Phan, and H. Srikanth, RSC Advances **6**, 38697 (2016).
[9] R. Das, N. Rinaldi-Montes, J. Alonso, Z. Amghouz, P. Gorria, J. A. Blanco, M. H. Phan, and H. Srikanth, ACS Applied Materials and Interfaces **8**, 25162 (2016).
[10] C. L. Dennis and R. Ivkov, Int. J. Hyperthermia **29**(8), 715 (2013).
[11] N. A. Usov and B. Ya. Liubimov, J. Appl. Phys. **112**, 023901 (2012).
[12] J. H. Lee, J. T. Jang, J. S. Choi, S. H. Moon, S. H. Noh, J. W. Kim, J. G. Kim, I. S. Kim, K. L. Park, and J. Cheon, Nat. Nanotechnol. **6**, 418 (2011).
[13] S. H. Moon, S. Noh, J.-H. Lee, T.-H. Shin, Y. Lim, and J. Cheon, Nano Lett. **17**, 800 (2017).
[14] V. Gavrilov-Isaac, S. Neveu, V. Dupuis, D. Taverna, A. Gloter, and V. Cabuil, Small **11**, 2614 (2015).
[15] S. Sun, H. Zeng, D. B. Robinson, S. Raoux, P. M. Rice, S. X. Wang, and G. Li, J. Am. Chem. Soc. **126**, 273 (2004).
[16] R. Das, J. Alonso, Z. N. Porshokouh, V. Kalappattil, D. Torres, M. H. Phan, E. Garaio, J. Á. García, J. L. S. Llamazares, and H. Srikanth, J. Phys. Chem. C **120**, 10086 (2016).
[17] J. Carrey *et al.*, J. Appl. Phys. **109**, 083921 (2011).
[18] R. Das *et al.*, AIP Advances (Submitted).
[19] I. Andreu, E. Natividad, L. Solozabal, and O. Robeau, ACS Nano **9**, 1408 (2015).